THE UNIVERSITY of EDINBURGH

Edinburgh Research Explorer

Numerical Simulation of String/Barrier Collisions: The Fretboard

Citation for published version:
Bilbao, S & Torin, A 2014, Numerical Simulation of String/Barrier Collisions: The Fretboard. in *Proceedings of the 17th International Conference on Digital Audio Effects.* Erlangen, Germany, 17th International Conference on Digital Audio Effects, Erlangen, Germany, 1/09/14.
<http://www.dafx14.fau.de/proceedings.html>

Link:
Link to publication record in Edinburgh Research Explorer

Document Version:
Publisher's PDF, also known as Version of record

Published In:
Proceedings of the 17th International Conference on Digital Audio Effects

General rights
Copyright for the publications made accessible via the Edinburgh Research Explorer is retained by the author(s) and / or other copyright owners and it is a condition of accessing these publications that users recognise and abide by the legal requirements associated with these rights.

Take down policy
The University of Edinburgh has made every reasonable effort to ensure that Edinburgh Research Explorer content complies with UK legislation. If you believe that the public display of this file breaches copyright please contact openaccess@ed.ac.uk providing details, and we will remove access to the work immediately and investigate your claim.

Download date: 30. Nov. 2021

NUMERICAL SIMULATION OF STRING/BARRIER COLLISIONS: THE FRETBOARD.

Stefan Bilbao, *

Acoustics and Audio Group
University of Edinburgh
Edinburgh, UK
sbilbao@staffmail.ed.ac.uk

Alberto Torin

Acoustics and Audio Group
University of Edinburgh
Edinburgh, UK
s1164558@sms.ed.ac.uk

ABSTRACT

Collisions play a major role in various models of musical instruments; one particularly interesting case is that of the guitar fretboard, the subject of this paper. Here, the string is modelled including effects of tension modulation, and the distributed collision both with the fretboard and individual frets, and including both effects of free string vibration, and under finger-stopped conditions, requiring an additional collision model. In order to handle multiple distributed nonlinearities simultaneously, a finite difference time domain method is developed, with a penalty potential allowing for a convenient model of collision within a Hamiltonian framework, allowing for the construction of stable energy-conserving methods. Implementation details are discussed, and simulation results are presented illustrating a variety of features of such a model.

1. INTRODUCTION

Physical modeling synthesis to date has relied, mainly, on linear models of distributed components, accompanied by pointwise nonlinearities often related to excitation mechanisms (such as, for example, models of the bow, hammer, or lip-reed interaction). See, e.g., [1] for an overview. In the pursuit of more realistic sound synthesis, recent research has focused on inherent nonlinearities in the distributed components themselves, beginning with the introduction of tension modulation effects in strings [2, 3, 4], shock wave effects in acoustic tubes [5], geometric nonlinearities in strings [6], and in 2D systems such as membranes and plates [7]. A distinct form of distributed nonlinearity, and one which is of great significance to models of strings is the contact between a distributed vibrating object with a rigid barrier.

The problem of the string in contact with a rigid barrier has seen research in the realm of musical acoustics for almost a century, going back to early investigations of Indian stringed instruments such as the sitar or tambura [8], and continuing to the present day, particularly using a geometric analysis for barriers of simplified forms [9, 10]. In practical sound synthesis applications, where the barrier may well be of a complex shape, and in musical acoustics investigations, more flexible methods have been employed, including digital waveguides [11, 12, 13, 14, 15], modal techniques [16], and time-stepping methods such as finite difference methods [11, 17, 14, 18].

The particular case of the interaction of a string with a fret, modelled as a lumped barrier element, in order to emulate realistic playing in fretted instruments such as the guitar has been researched by Evangelista [12, 19], which is the case of interest in this paper. Here, a distributed view of the barrier is taken, including frets and the backing fretboard. Finite difference time domain methods are employed, with special attention paid to the problem of numerical stability, which is especially pronounced here, due to the inherently non-smooth form of the collision interaction. To this end, a formalism based upon the use of an added potential, allowing the use of a Hamiltonian framework, but permitting some spurious penetration of the string into the barrier is employed. The action of a stopping finger, in order to simulate finger motion against the fretboard, is also included here. The model here is complementary to that of Evangelista mentioned above, in that here, string motion is taken to be perpendicular to the fretboard—in a full model, both polarizations need to be taken into account. Finger plucking interactions have been described previously—see, e.g., [20]

Section 2 presents a complete model of string vibration in a single polarization, including tension modulation effects, distributed collision against a barrier of arbitrary shape, a plucking excitation, as well as a further collision due to stopping of a finger against the fretboard. An energy analysis completes this section. Section 3 is a concise presentation of finite difference time domain construction, with a discussion of numerical stability, arrived at through an analogous energy analysis, and implementation issues, and in particular a vector nonlinear equation to be solved at each time step. Simulation results, illustrating various features of such a model, are presented in Section 4. Sound synthesis examples are available online at `http://www.ness-music.eu`

2. STRING MODEL

A model of constrained string vibration may be written in a compact form as

$$\rho\partial_{tt}u = \mathcal{L}[u] + \mathcal{K}[u] + \mathcal{F}_e + \mathcal{F}_c - \mathcal{F}_f \qquad (1)$$

Here, $u(x,t)$ is the transverse displacement of a string in a single polarization (assumed here to be perpendicular to a constraining surface, to be described shortly), as a function of time $t \geq 0$ and $x \in \mathcal{D} = [0, L]$, where L is string length when at rest. The string is of linear mass density ρ kg/m, and ∂_{tt} represents double partial differentiation with respect to time t. See Figure 1. Because this model of a string is in a single polarization only, it is thus capable of modelling only string plucks perpendicular to the fretboard—which is a great simplification from the true situation, but one allowing for an analysis of many of the important features of such an instrument.

The linear operator $\mathcal{L}$ is defined, in terms of its action on the function u, as

$$\mathcal{L}[u] = \left(T\partial_{xx} - EI\partial_{xxxx} - 2\sigma_0\rho\partial_t + 2\sigma_1\rho\partial_{txx}\right)u \qquad (2)$$

* This work was supported by the European Research Council, under grant number StG-2011-279068-NESS.

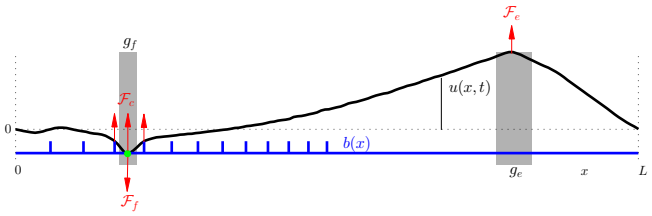

Figure 1: *Diagram of string, of displacement $u(x,t)$, in contact with a barrier $b(x)$, as indicated in blue. An excitation force density $\mathcal{F}_e$ is applied over a distribution g_e, and a force density $\mathcal{F}_f$ is applied by a finger (indicated in green) over a distribution g_f. A collision force density $\mathcal{F}_c$ results at points of contact between the string and barrier.*

and describes the linear dynamics of the string, where partial differentiation with respect to x is indicated by ∂_x. The four terms model, respectively, string tension, stiffness, frequency-independent loss, and frequency-dependent loss. Here, T is string tension, in N, E is Young's modulus, in Pa, I is the string moment of inertia (and equal to $\pi r^4/4$, for a string of circular cross-section and radius r m), and σ_0 and σ_1 are loss parameters, which may be set according to comparison with measured data. Such a linear model is relatively standard in the musical acoustics literature (with some variation in the way in which the frequency-dependent loss terms are modelled [21, 22]).

The nonlinear operator $\mathcal{K}$ is defined as

$$\mathcal{K}[u] = \frac{EA}{2L}\left(\int_{\mathcal{D}} (\partial_x u)^2 \, dx\right) \partial_{xx} u \tag{3}$$

where A is the string cross-sectional area in m^2, and describes effects of tension modulation in the string, giving rise to variations in pitch with excitation amplitude, or pitch glides; such a model is due to Kirchhoff [23] and Carrier [24], and has seen extensive use in sound synthesis applications [2, 3, 4, 25]. This is a particularly simple form of string nonlinearity—more realistic effects, including the generation of phantom partials [26, 6], may be obtained using a complete form which models the coupling between transverse and longitudinal motion in the string.

The final three terms in (1) represent force densities due, respectively, to a plucking action, collision of the string with the fretboard, and the stopping motion of a finger, and will be defined in the following sections.

2.1. Excitation

A relatively simple model of excitation will be employed here, namely that of a force density

$$\mathcal{F}_e = g_e f_e$$

where here, $f_e(t)$ is an applied force in N, and where $g_e(x)$ is a distribution selecting the region of application of the excitation (chosen normalized, with $\int_{\mathcal{D}} g_e \, dx = 1$, and perhaps as a Dirac delta function $g_e(x) = \delta(x - x_e)$, for a plucking point $x = x_e$). In some models of plucking excitation [27], a relatively smooth form of excitation function is employed:

$$f_e(t) = \begin{cases} \frac{f_p}{2}\left(1 - \cos(\pi(t - t_0)/t_p)\right) & t_0 \le t \le t_p \\ 0 & \text{else} \end{cases} \tag{4}$$

This function is characterized by a small set of parameters, namely: start time t_0, duration t_p, and maximum force f_p.

One could go further here and specify a full model of the plucking finger, but as this is not the focus of this paper, and also because in general, the duration of a pluck is extremely short (on the order of 1-10 ms) the simple form above will be employed, as in previous work on guitar synthesis [28]. More involved models are available—see, e.g., [29, 30].

2.2. The Fretboard

The string is assumed to vibrate above a rigid barrier of height $b(x)$—in the case of a fretboard, the function will include the profile of the board itself, as well as pointwise protuberances (the frets themselves). To this end, suppose that the function is of the form $b(x) = b_{back}(x)$, almost everywhere, where $b_{back}(x)$ is a smooth function representing the fretboard itself, in the absence of the frets. At locations x_m, $m = 1, \ldots, N_{fret}$ at which the N_{fret} frets are located, the function takes on the values $b(x_m) = b_{fret}^{(m)}$. See Figure 1.

The force density $\mathcal{F}_c$ acts upwards on the string, and may be defined in terms of a potential density $\Phi_c \ge 0$ as

$$\mathcal{F}_c = \frac{\partial_t \Phi_c}{\partial_t \eta_c} \qquad \text{where} \qquad \eta_c = b - u \tag{5}$$

The potential $\Phi_c(\eta_c)$ here is to be viewed as a penalty density, active whenever and wherever η_c, the difference between the barrier height and string height is positive, implying interpenetration, and thus repelling the string. A useful form of the penalty potential Φ_c is of the form of a power law $\Phi_c = \Phi_{K,\alpha}(\eta_c)$, where, for a value or distribution p

$$\Phi_{K,\alpha}(p) = \frac{K}{\alpha + 1}[p]_+^{\alpha+1} \qquad [p]_+ = \frac{1}{2}(p + |p|)$$

where $K \ge 0$, and $\alpha \ge 1$. In simulation, the degree of interpenetration can be controlled through a proper choice of K and α—see Section 4.2. Note that, under this choice of the potential, $\mathcal{F}_c = K[\eta_c]_+^{\alpha}$, and so this collision model is of a form similar to that seen in lumped models of impact, such as that of Hertz [31], and commonly used in models of striking action in musical instruments [22, 32]; here, however, it is to be viewed as an approximation to an ideal elastic collision. The form in (5), written in terms of a potential, however, is more useful when it comes to simulation design—see Section 3.

2.3. Finger-stopping

Another separate collision which must be taken into account in a full articulated model of such a stringed instrument is the action of a stopping finger pressing the string against the frets or fretboard. This collision is slightly different from the case of the barrier/string collision described in the previous section, as the finger must be permitted its own dynamics, including damping effects, and is subject to external control. In this case, where the string is assumed to move transverse to the fretboard, rubbing friction effects against the fret are not included—see [12].

For a lumped model of such a finger, the force density $\mathcal{F}_f$, now acting downward on the string from above, may be written as

$$\mathcal{F}_f = g_f f_f$$

Here, $g_f = g_f(x,t)$ is an externally specified function representing the region of contact of the finger with the string at time t, again chosen normalized, with $\int_{\mathcal{D}} g_f \, dx = 1$, and f_f is the force applied to the string, in N. The position of the finger, u_f, may be described by

$$M_f \frac{d^2 u_f}{dt^2} = f_f - f_0$$

where here, M_f is the finger mass, in kg, and where $f_0 = f_0(t)$ is an external force signal supplied by the player.

As in the case of the string/barrier collision, the interaction force f_f depends on a measure η_f of the relative displacement between the string and finger at the stopping location:

$$f_f = \frac{d\Phi_f/dt}{d\eta_f/dt} + \frac{d\eta_f}{dt}\Xi_f \qquad \eta_f = \int_{\mathcal{D}} g_f u \, dx - u_f \quad (6)$$

Here again, $\Phi_f(\eta_f) \geq 0$ is a collision potential—now, however, it is intended to model elastic deformation of the finger under the pressing action; the model here is identical to that of a striking piano hammer, with losses taken into account, and under a continuous excitation force. As in the case of the hammer, a choice of collision potential $\Phi_f = \Phi_{K_f,\alpha_f}(\eta_f)$ is reasonable, where again $K_f \geq 0$ and $\alpha_f \geq 1$. Also modelled here are losses, through a function $\Xi_f(\eta_f) \geq 0$. The model of Hunt and Crossley [33] is appropriate here, with $\Xi_f = \Xi_{K_f,\alpha_f,\beta_f}$, where

$$\Xi_{K_f,\alpha_f,\beta_f}(\eta_f) = \beta_f K_f \frac{d\eta_f}{dt} [\eta_f]_+^{\alpha}$$

for some constant $\beta_f \geq 0$.

2.4. Energy Balance

System (1) includes three separate nonlinearities, due to tension modulation, collision, and finger stopping, as well as non-autonomous time variation due to the finger-stopping distribution g_f, and thus frequency-domain analysis will thus be of virtually no use in designing a numerical method. To this end, it is useful to present an energy balance for the system.

It may be easily verified, through the multiplication of (1) by $\partial_t u$, integrating over the domain $\mathcal{D}$, and employing integration by parts, that the complete model described above satisfies an energy balance of the form

$$\frac{d\mathfrak{H}}{dt} = -\mathfrak{Q} + \mathfrak{P} + \mathfrak{B} \quad (7)$$

where here, at time t, $\mathfrak{H}(t)$ represents the total stored energy of the system, $\mathfrak{Q}(t)$ is total dissipated power, $\mathfrak{P}(t)$ is input power, and $\mathfrak{B}$ represents energy supplied to the string at the boundaries at $x = 0$ and $x = L$.

In particular,

$$\begin{aligned} \mathfrak{H} &= \mathfrak{H}_L + \mathfrak{H}_K + \mathfrak{H}_c + \mathfrak{H}_f \\ \mathfrak{Q} &= \mathfrak{Q}_L + \mathfrak{Q}_f \\ \mathfrak{P} &= \mathfrak{P}_e + \mathfrak{P}_f \end{aligned}$$

where, for the stored energy terms corresponding to linear string vibration, nonlinear string vibration, the collision interaction, and the finger interaction, respectively, one has

$$\begin{aligned} \mathfrak{H}_L &= \int_{\mathcal{D}} \frac{\rho}{2} (\partial_t u)^2 + \frac{T}{2} (\partial_x u)^2 + \frac{EI}{2} (\partial_{xx} u)^2 \, dx \\ \mathfrak{H}_K &= \frac{EA}{8L} \left(\int_{\mathcal{D}} \partial_x u \, dx \right)^2 \\ \mathfrak{H}_c &= \int_{\mathcal{D}} \Phi_c \, dx \\ \mathfrak{H}_f &= \frac{M_f}{2} \left(\frac{du_f}{dt} \right)^2 + \Phi_f \end{aligned}$$

For the individual power loss terms $\mathfrak{Q}_L$ and $\mathfrak{Q}_f$ in the string and finger, respectively, one has

$$\begin{aligned} \mathfrak{Q}_L &= \int_{\mathcal{D}} 2\rho\sigma_0 (\partial_t u)^2 + 2\rho\sigma_1 (\partial_{tx} u)^2 \, dx \\ \mathfrak{Q}_f &= \left(\frac{d\eta_f}{dt} \right)^2 \Xi_f(\eta_f) \end{aligned}$$

For the supplied power terms $\mathfrak{P}_e$ and $\mathfrak{P}_f$ from the excitation and stopping finger, respectively, one has

$$\begin{aligned} \mathfrak{P}_e &= f_e \int_{\mathcal{D}} g_e \partial_t u \, dx \\ \mathfrak{P}_f &= f_f \int_{\mathcal{D}} u \partial_t g_f \, dx - \frac{du_f}{dt} f_0 \end{aligned}$$

The boundary power term $\mathfrak{B}$ is given by

$$\begin{aligned} \mathfrak{B} = &\left(T + \frac{EA}{2L} \left(\int_{\mathcal{D}} \partial_x u \, dx \right)^2 \right) \partial_t u \partial_x u \\ &- EI \left(\partial_t u \partial_{xxx} u - \partial_{tx} u \partial_{xx} u \right) - 2\rho\sigma_1 \partial_t u \partial_{xt} u \big|_{x=0}^{x=L} \end{aligned}$$

In this study, boundary conditions are chosen as simply supported (i.e., $u = \partial_{xx} u = 0$ at $x = 0$ and $x = L$), and thus $\mathcal{B}$ vanishes identically.

Under unforced conditions (i.e., with no excitation force f_e, no applied finger stopping force f_0, and no time variation of the stopping finger distribution g_f), note that $\mathfrak{H} \geq 0$, and $\mathfrak{Q} \geq 0$, and thus, for all $t \geq 0$

$$\frac{d\mathfrak{H}}{dt} \leq 0 \qquad \longrightarrow \qquad 0 \leq \mathfrak{H}(t) \leq \mathfrak{H}(0)$$

and the system as a whole is dissipative. If, furthermore, loss is not present (i.e., if $\sigma_0 = \sigma_1 = \Xi_f = 0$), then the system is exactly lossless. Such an energy balance serves as a useful design principle in arriving at numerically stable simulation methods. See Section 3.

3. TIME STEPPING METHODS

In this section, the basic techniques underlying the construction of time-domain finite difference schemes are presented, in a condensed vectorized form. For a more expanded treatment of such methods, see, e.g., [34], or, in the context of physical modeling synthesis, [35].

3.1. Grid Functions and Difference Operators

The grid function u_l^n, for integer $n \geq 0$ and $l = 0, \ldots, N$, represents an approximation to the function $u(x,t)$ at time $t = nk$ and $x = lh$. Here, k is the time step (and $f_s = 1/k$ is the sample rate, chosen a priori), and h is the grid spacing, chosen such that it divides the length L evenly as $N = L/h$.

In this case, where the system under study is 1D, and because the boundary conditions are of simple form (that is, simply supported), it is useful to move directly to a vector representation of the state, namely the column vector $\mathbf{u}^n = [u_1^n, \ldots, u_{N-1}^n]^T$. Here, the values u_0^n and u_N^N have been omitted from the vector form, and thus need not be calculated, as they are identically zero—this choice has implications for the matrix representations of various spatial difference operators, as will be described shortly.

For any vector $\mathbf{w}^n$, unit time shifts e_{t+} and e_{t-} are defined as

$$e_{t+}\mathbf{w}^n = \mathbf{w}^{n+1} \qquad e_{t-}\mathbf{w}^n = \mathbf{w}^{n-1}$$

The forward, backward and centered difference approximations to a first time derivative may thus be defined as

$$\delta_{t+} = \frac{e_{t+} - 1}{k} \quad \delta_{t-} = \frac{1 - e_{t-}}{k} \quad \delta_{t\cdot} = \frac{e_{t+} - e_{t-}}{2k} \tag{8}$$

and time averaging operators as

$$\mu_{t+} = \frac{e_{t+} + 1}{2} \quad \mu_{t-} = \frac{1 + e_{t-}}{2} \quad \mu_{t\cdot} = \frac{e_{t+} + e_{t-}}{2} \tag{9}$$

An approximation to a second time derivative follows as

$$\delta_{tt} = \delta_{t+}\delta_{t-} = \frac{e_{t+} - 2 + e_{t-}}{k^2} \tag{10}$$

Forward and backward approximations to spatial differentiation ∂_x, when applied to the grid function $\mathbf{u}^n$, and taking into account the simply supported boundary condition, may be written in matrix form as $\mathbf{D}_{x+}$ and $\mathbf{D}_{x-}$, where $\mathbf{D}_{x+}$ is an $N \times (N-1)$ matrix, and $\mathbf{D}_{x-}$ is $(N-1) \times N$:

$$\mathbf{D}_{x+} = \frac{1}{h}\begin{bmatrix} 1 & & & & \\ -1 & 1 & & & \\ & \ddots & \ddots & & \\ & & & -1 & 1 \\ & & & & -1 \end{bmatrix} \qquad \mathbf{D}_{x-} = -\mathbf{D}_{x+}^T$$

where ^{T} indicates the transpose operation.

Approximations to the second and fourth spatial derivative, $\mathbf{D}_{xx}$ and $\mathbf{D}_{xxxx}$ respectively, both $(N-1) \times (N-1)$ matrices, may be written, under simply supported conditions, as

$$\mathbf{D}_{xx} = \mathbf{D}_{x-}\mathbf{D}_{x+} \qquad \mathbf{D}_{xxxx} = \mathbf{D}_{xx}\mathbf{D}_{xx}$$

3.2. Finite Difference Scheme

A finite difference time domain scheme for (1) may then be written, in vector-matrix form, in terms of the grid function $\mathbf{u}^n$, as

$$\rho\delta_{tt}\mathbf{u}^n = \mathfrak{l}[\mathbf{u}^n] + \mathfrak{k}[\mathbf{u}^n] + \mathfrak{f}_e^n + \mathfrak{f}_c^n - \mathfrak{f}_f^n \tag{11}$$

Here, in analogy with definition (2) for the linear operator $\mathcal{L}$, the linear discrete operator $\mathfrak{l}$ is defined as

$$\mathfrak{l}[\mathbf{u}^n] = (T\mathbf{D}_{xx} - EI\mathbf{D}_{xxxx} - 2\sigma_0\rho\delta_{t\cdot} + 2\sigma_1\rho\delta_{t-}\mathbf{D}_{xx})\,\mathbf{u}^n \tag{12}$$

and the nonlinear operator $\mathfrak{k}$ as

$$\mathfrak{k}[\mathbf{u}^n] = \frac{EAh}{2L}\left(\mathbf{D}_{x+}\mathbf{u}^n\right)^T\left(\mu_{t\cdot}\mathbf{D}_{x+}\mathbf{u}^n\right)\mathbf{D}_{xx}\mathbf{u}^n \tag{13}$$

Note the use of the time averaging operator $\mu_{t\cdot}$ in (13) above, necessary in arriving at a stable scheme [36].

3.3. Discrete Force Densities

The discrete force density terms $\mathfrak{f}_e^n$, $\mathfrak{f}_c^n$ and $\mathfrak{f}_f^n$ given in (11) are all $(N-1)$ element column vectors.

The discrete force excitation density $\mathfrak{f}_e^n$ may be written as $\mathfrak{f}_e^n = \mathbf{g}_e f_e^n$ where $\mathbf{g}_e$ corresponds to $g_e(x)$, with $h\mathbf{1}^T\mathbf{g}_e = 1$, where $\mathbf{1}$ is an $N-1$ element column vector consisting of ones, and where f_e^n is sampled from $f_e(t)$, as defined in (4).

The discrete collision force due to the interaction with the barrier $\mathfrak{f}_c^n$ requires a more detailed treatment. Because one would like to model collision between the string and the fretboard at the $N-1$ grid points at which the string is defined, and also at the N_{fret} locations at which the frets themselves are defined (which, in general, do not lie at grid locations), it is useful to write $\mathfrak{f}_c^n = \mathbf{G}_c\mathbf{f}_c^n$, where $\mathbf{f}_c$ is an $N_c = N - 1 + N_{fret}$ element force vector, and $\mathbf{G}_c$ is an $(N-1) \times N_c$ matrix interpolant. In particular, $\mathbf{G}_c = \frac{1}{h}[\mathbf{I}_{N-1}|\mathbf{G}_{fret}]$, where $\mathbf{I}_{N-1}$ is the $(N-1) \times (N-1)$ identity matrix, and where $\mathbf{G}_{fret}$ is an $(N-1) \times N_{fret}$ matrix, the mth column of which is an interpolant to the mth fret location x_m. Any form of interpolant (i.e., bilinear, Lagrangian, etc.) may be employed in this construction.

For the collision itself, one may then write, in analogy with (5),

$$\mathbf{f}_c^n = \frac{\delta_{t\cdot}\Phi_c^n}{\delta_{t\cdot}\eta_c^n} \qquad \eta_c^n = \mathbf{b} - h\mathbf{G}_c^T\mathbf{u}^n \tag{14}$$

in terms of the N_c element vectors Φ_c^n, η_c^n and $\mathbf{b}^n$. This latter vector, representing the barrier profile, may be decomposed as $\mathbf{b} = [\mathbf{b}_{back}^T|\mathbf{b}_{fret}^T]^T$, where $\mathbf{b}_{back}$ is the $N-1$ element column vector consisting of samples of the fretboard profile $b(x)$ at the grid locations, and $\mathbf{b}_{fret}$ is an N_{fret} element column vector consisting of the fret heights $b_{fret}^{(m)}$, $m = 1, \ldots, N_{fret}$. As in the continuous case, a power law potential may be employed, such that $\Phi_c^n = \Phi_{K,\alpha}(\eta_c^n)$. (Here and henceforth, expressions such as the first in (14) represent a vector resulting from element-by-element division of two vectors.)

The finger force density $\mathfrak{f}_f^n$ may be written as $\mathfrak{f}_f^n = \mu_{t\cdot}\left(\mathbf{g}_f^n\right) f_f^n$, where as in the case of the excitation, $\mathbf{g}_f^n$ is an $N-1$ element normalized column vector—note in particular that it is time-varying, allowing for gestural control of the finger-stopping action. The finger force may be discretized, in analogy with (6), as

$$f_f^n = \frac{\delta_{t\cdot}\Phi_f^n}{\delta_{t\cdot}\eta_f^n} + \delta_{t\cdot}\eta_f^n\Xi_f^n \qquad \eta_f^n = h\left(\mathbf{g}_f^n\right)^T\mathbf{u}^n - u_f^n \tag{15}$$

where $\Phi_f^n = \Phi_{K_f,\alpha_f}(\eta_f^n)$, and where $\Xi_f^n = \Xi_{K_f,\alpha_f,\beta_f}(\eta_f^n)$. Finally, the equation of motion of the finger, in terms of displacement u_f^n may be written as

$$M_f\delta_{tt}u_f^n = f_f^n - f_0^n$$

3.4. Discrete Energy Balance and Stability Conditions

In analogy with the energy balance (7) for the continuous system, a discrete energy balance follows for the scheme presented in Section 3.2:

$$\delta_{t-}\mathfrak{h}^{n+1/2} = -\mathfrak{q}^n + \mathfrak{p}^n + \mathfrak{b}^n \tag{16}$$

where here, $\mathfrak{h}^{n+1/2}$ represents the total stored energy of the system (written here as interleaved with respect to values calculated in the scheme itself), $\mathfrak{q}^n$ is total dissipated power, $\mathfrak{p}^n$ is input power, and $\mathfrak{b}^n$ represents energy supplied to the string at the boundaries at $l = 0$ and $l = N$—in this case, $\mathfrak{b}^n = 0$ by construction, so may be safely ignored in the remainder of this analysis. Here, the various terms may be decomposed as

$$\begin{aligned}\mathfrak{h}^{n+1/2} &= \mathfrak{h}_L^{n+1/2} + \mathfrak{h}_K^{n+1/2} + \mathfrak{h}_c^{n+1/2} + \mathfrak{h}_f^{n+1/2} \\ \mathfrak{q}^n &= \mathfrak{q}_L^n + \mathfrak{q}_f^n \\ \mathfrak{p}^n &= \mathfrak{p}_e^n + \mathfrak{p}_f^n\end{aligned}$$

where, for the stored energy terms corresponding to linear string vibration, nonlinear string vibration, the collision interaction, and the finger interaction, respectively, one has

$$\begin{aligned}\mathfrak{h}_L^{n+1/2} &= \frac{\rho h}{2}|\delta_{t+}\mathbf{u}^n|^2 + \frac{Th}{2}\left(\mathbf{D}_{x+}\mathbf{u}^n\right)^T \mathbf{D}_{x+}\mathbf{u}^{n+1} \\ &\quad + \frac{EIh}{2}\left(\mathbf{D}_{xx}\mathbf{u}^n\right)^T \mathbf{D}_{xx}\mathbf{u}^{n+1} - \frac{\rho\sigma_1 hk}{2}|\delta_{t+}\mathbf{D}_{x+}\mathbf{u}^n|^2 \\ \mathfrak{h}_K^{n+1/2} &= \frac{EAh^2}{8L}\left(\left(\mathbf{D}_{x+}\mathbf{u}^n\right)^T \mathbf{D}_{x+}\mathbf{u}^{n+1}\right)^2 \\ \mathfrak{h}_c^{n+1/2} &= \mathbf{1}^T \mu_{t+}\Phi_c^n \\ \mathfrak{h}_f^{n+1/2} &= \frac{M_f}{2}\left(\delta_{t+}u_f^n\right)^2 + \Phi_f^n\end{aligned}$$

and for the power loss terms,

$$\begin{aligned}\mathfrak{q}_L^n &= 2\rho\sigma_0 h|\delta_{t\cdot}\mathbf{u}^n|^2 + 2\rho\sigma_1 h|\delta_{t\cdot}\mathbf{D}_{x+}\mathbf{u}^n|^2 \\ \mathfrak{q}_f &= \left(\delta_{t\cdot}\eta_f^n\right)^2 \Xi_f^n\end{aligned}$$

For the supplied power terms $\mathfrak{p}_e^n$ and $\mathfrak{p}_f^n$ from the excitation and stopping finger, respectively, one has

$$\begin{aligned}\mathfrak{p}_e^n &= f_e^n h\left(\delta_{t\cdot}\mathbf{u}^n\right)^T \mathbf{g}_e \\ \mathfrak{p}_f^n &= f_f^n h\left(\mu_{t\cdot}\mathbf{u}^n\right)^T \delta_{t\cdot}\mathbf{g}_f^n - \delta_{t\cdot}u_f^n f_0^n\end{aligned}$$

Considering the discrete power balance (16), under unforced conditions (i.e., $\mathfrak{p}_e^n = \mathfrak{p}_f^n = 0$), note that the loss terms $\mathfrak{q}_L^n$ and $\mathfrak{q}_f^n$ are non-negative; the only stored energy term which is not non-negative is that corresponding to the string energy $\mathfrak{h}_L$. It is straightforward to show [35] that under the condition $h \geq h_{min}$, where

$$h_{min}^2 = \frac{k}{2}\left(\frac{Tk}{\rho} + 4\sigma_1 + \sqrt{\left(\frac{Tk}{\rho} + 4\sigma_1\right)^2 + \frac{16EI}{\rho}}\right) \quad (17)$$

the term $\mathfrak{h}_L$ is non-negative; this condition serves as a stability condition for the entire scheme. Again, under lossless conditions (i.e., with $\sigma_0 = \sigma_1 = \Xi^n = 0$), the scheme is numerically lossless. See Section 4.4. Notice that condition (17) is equivalent to that arrived at using von Neumann analysis [34] for the linear string in isolation, though now for the complete system involving multiple nonlinearities.

3.5. Vector-matrix Update Form

In the interest of illustrating how such a scheme may be used in practice, it is useful to rewrite it in a vector-matrix update form as

$$\mathbf{A}^n\mathbf{u}^{n+1} = \mathbf{B}\mathbf{u}^n + \mathbf{C}^n\mathbf{u}^{n-1} + \mathbf{j}_e f_e^n + \mathbf{J}^n\mathbf{f}^n \quad (18)$$

where here, $\mathbf{A}^n$, $\mathbf{B}$ and $\mathbf{C}^n$ are $(N-1)\times(N-1)$ matrices defined as

$$\begin{aligned}\mathbf{A}^n &= \left(1 + \sigma_0 k\right)\mathbf{I}_{N-1} + \left(\mathbf{a}^n\right)\left(\mathbf{a}^n\right)^T \\ \mathbf{B} &= 2\mathbf{I}_{N-1} + \left(\frac{k^2T}{\rho} + 2\sigma_1 k\right)\mathbf{D}_{xx} - \frac{EIk^2}{\rho}\mathbf{D}_{xxxx} \\ \mathbf{C}^n &= \left(\sigma_0 k - 1\right)\mathbf{I}_{N-1} - \left(\mathbf{a}^n\right)\left(\mathbf{a}^n\right)^T - 2\sigma_1 k\mathbf{D}_{xx}\end{aligned}$$

Due to the tension modulation nonlinearity, $\mathbf{A}^n$ and $\mathbf{C}^n$ are dependent on previously computed state values through the column vector $\mathbf{a}^n$, defined as

$$\mathbf{a}^n = \frac{k}{2}\sqrt{\frac{EAh}{\rho L}}\mathbf{D}_{xx}\mathbf{u}^n$$

The vector $\mathbf{j}_e$ is defined as $\mathbf{j}_e = k^2\mathbf{g}_e/\rho$, and $\mathbf{f}^n = [(\mathbf{f}_c^n)^T\,|f_f^n]^T$ is the consolidation of the contact forces due to the barrier and finger, with the combined matrix $\mathbf{J}^n$ given by $\mathbf{J}^n = k^2\mathbf{G}^n/\rho$, where $\mathbf{G}^n = [\mathbf{G}_c|-\mathbf{g}_f^n]$. Notice that $\mathbf{J}^n$ and $\mathbf{G}^n$ include effects of time variation due to the motion of the stopping finger.

The update form (18) requires the determination of the collision force vector $\mathbf{f}^n$; to this end, it may be rewritten as

$$\mathbf{u}^{n+1} = \mathbf{q}^n + \tilde{\mathbf{J}}^n\mathbf{f}^n \quad (19)$$

where

$$\mathbf{q}^n = \left(\mathbf{A}^n\right)^{-1}\left(\mathbf{B}\mathbf{u}^n + \mathbf{C}^n\mathbf{u}^{n-1} + \mathbf{j}_e f_e^n\right) \quad \tilde{\mathbf{J}}^n = \left(\mathbf{A}^n\right)^{-1}\mathbf{J}$$

Though the calculation of $\mathbf{q}^n$ and $\tilde{\mathbf{J}}^n$ might appear to require the full inversion of a matrix $\mathbf{A}^n$ (or at least a linear system solution), note that $\mathbf{A}^n$ is a rank one perturbation of a scaled identity matrix, and thus the inverse may be written directly, using the Sherman-Morrison-Woodbury formula [37] as

$$\left(\mathbf{A}^n\right)^{-1} = \frac{1}{1+\sigma_0 k}\left(\mathbf{I}_{N-1} - \frac{\left(\mathbf{a}^n\right)\left(\mathbf{a}^n\right)^T}{1 + \sigma_0 k + \left(\mathbf{a}^n\right)^T\left(\mathbf{a}^n\right)}\right)$$

which leads to a matrix multiplication with $O(N)$ operations.

3.6. A Nonlinear Equation

Define the set of collision distances η^n as $\eta^n = [(\eta_c^n)^T\,|\eta_f^n]^T$. From the definitions (14) and (15), one then has

$$\eta^n = \begin{bmatrix}\mathbf{b} \\ -u_f^n\end{bmatrix} - h\mathbf{G}^n\mathbf{u}^n$$

From this, one may further define the vector $\mathbf{r}^n = [(\mathbf{r}_c^n)^T\,|r_f^n]^T$ as $\mathbf{r}^n = \eta^{n+1} - \eta^{n-1}$, and $\mathbf{r}^n$ may be written as

$$\mathbf{r}^n = \gamma^n - \mathbf{Z}\mathbf{f}^n - h\left(\left(\mathbf{G}^{n+1}\right)^T\mathbf{u}^{n+1} - \left(\mathbf{G}^{n-1}\right)^T\mathbf{u}^{n-1}\right) \quad (20)$$

where

$$\gamma^n = \begin{bmatrix}\mathbf{0}_{N_c,1} \\ -2\left(u_f^n - u_f^{n-1}\right) + \frac{k^2}{M_f}f_0^n\end{bmatrix}$$

where $\mathbf{0}_{N_c,1}$ is an N_c element column vector, and $\mathbf{Z}$ is an $(N_c+1)\times(N_c+1)$ matrix, all zero, except for a value of k^2/M_f as the entry at the lower right corner.

For the forces, from the definitions (14) and (15), one has

$$\mathbf{f}^n = \mathbf{\Lambda}^n + \mathbf{P}^n\mathbf{r}^n \quad (21)$$

where $\mathbf{\Lambda}^n$ is a diagonal $(N_c+1)\times(N_c+1)$ matrix with diagonal entries given by $\mathrm{diag}\left(\mathbf{\Lambda}^n\right) = [(\lambda_c^n)^T\ |\lambda_f^n]^T$, with

$$\lambda_c^n = \frac{\phi_c\left(\mathbf{r}_c^n + \eta_c^{n-1}\right) - \phi_c\left(\eta_c^{n-1}\right)}{\mathbf{r}_c^n}$$

and

$$\lambda_f^n = \frac{\phi_f\left(r_f^n + \eta_f^{n-1}\right) - \phi_f\left(\eta_f^{n-1}\right)}{r_f^n}$$

and where $\mathbf{P}^n$ is an $(N_c+1)\times(N_c+1)$ matrix, all zero except for a value of $\Xi_f^n/(2k)$ in the lower right hand entry.

Finally, (19), (20) and (21) may be consolidated into a single vector nonlinear equation as

$$\mathbf{Q}^n\mathbf{r}^n + \mathbf{M}^n\Lambda^n + \mathbf{l}^n = \mathbf{0}$$

where

$$\begin{aligned}\mathbf{M}^n &= \mathbf{Z}^n + h\left(\mathbf{G}^{n+1}\right)^T\tilde{\mathbf{J}}^n\\ \mathbf{Q}^n &= \mathbf{I}_{N_c+1} + \mathbf{M}^n\mathbf{P}^n\\ \mathbf{l}^n &= -\gamma^n + h\left(\mathbf{G}^{n+1}\right)^T\mathbf{q}^n - h\left(\mathbf{G}^{n-1}\right)^T\mathbf{u}^{n-1}\end{aligned}$$

Numerically, such an equation may be solved using an iterative method such as, e.g., Newton-Raphson.

4. SIMULATION RESULTS

In this section, various features of simulations for the system described above are explored.

4.1. Visualization: Free Vibration

As a first example, consider a string positioned above a fretboard and a series of 12 frets, under a plucking action—see Figure 2, showing the time evolution of the string profile under different plucking forces. In one case, the string vibration is free from collision, but in the other, it is sufficient to allow for rebounding against the frets, greatly distorting the profile of the string subsequently. It should be noted that under normal lossy conditions, string vibration amplitude is decreased over time, and thus the collision with the fretboard will lead to transients; similarly, stiffness effects in the string lead to dispersion, also decreasing the maximum string displacement after the initial pluck.

4.2. Spurious Penetration

The penalty potential formulation intended to model the rigid collision between string and fretboard allows some unphysical penetration of the string into the fretboard itself. One question which emerges is then: how large is this penetration? For the plucked excitation simulation described in the previous section, the maximum penetration over the length of the string is plotted as a function of time step in Figure 3—in this case, it takes on values under 10^{-9} m, which is definitely acceptable in any acoustics simulation. The degree of penetration may be controlled through the choice of K—the larger it is, the less the penetration, with the side effect that the number of iterations required in Newton's method tends to increase. See Section 5 for more commentary on this point.

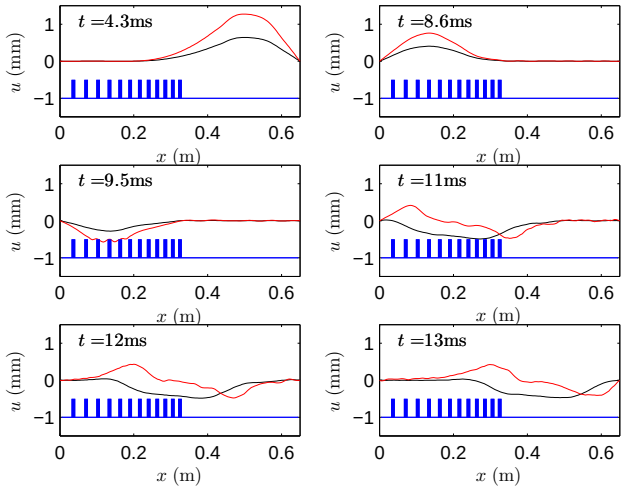

Figure 2: *Time evolution of the profile of a string in contact with a fretboard (in blue), under plucking excitations of different amplitudes—in black, with a maximal excitation of $f_p = 0.5$ N, and in red, with $f_p = 1$ N. In this case, the string is of parameters $L = 0.65$ m, $\rho = 5.25\times10^{-3}$ kg/m, $T = 60$ N, $E = 2\times10^{11}$ Pa, with radius $r = 4.3\times10^{-4}$ m, and loss parameters $\sigma_0 = 1.38$ and $\sigma_1 = 1.25\times10^{-4}$. The barrier collision parameters are $K = 10^{15}$ and $\alpha = 2.3$, and the pluck occurs pointwise at location $x = 0.52$ m. The sample rate is 88.2 kHz.*

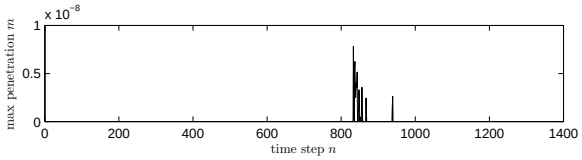

Figure 3: *Maximal penetration, in m, as a function of time step n, for the simulation described in Section 4.1.*

4.3. Visualization: Finger Tap

As a further example, consider the string under the application of a tapping gesture on the fretboard, as illustrated in Figure 4. In this case, the tapping is modelled (crudely!) as an unforced finger with an initial velocity rebounding from the string, accompanied by an intermediate pinning action against the fretboard itself. See Figure 4, illustrating the interaction of the finger with a string backed by a fretboard and a series of 12 frets, with parameters for the string and finger as given in the caption.

4.4. Energy Partition

In this example, the system has been assumed lossless, such that a plot of the energy partition for the system over time may be shown, as in Figure 5 at left; the finger energy is transferred first to the linear and nonlinear energy components of the string, then to the stored energy of the collision, when the string is in contact with the fretboard, and finally fully back to the finger, which rebounds with a speed identical to its initial speed. Notice in

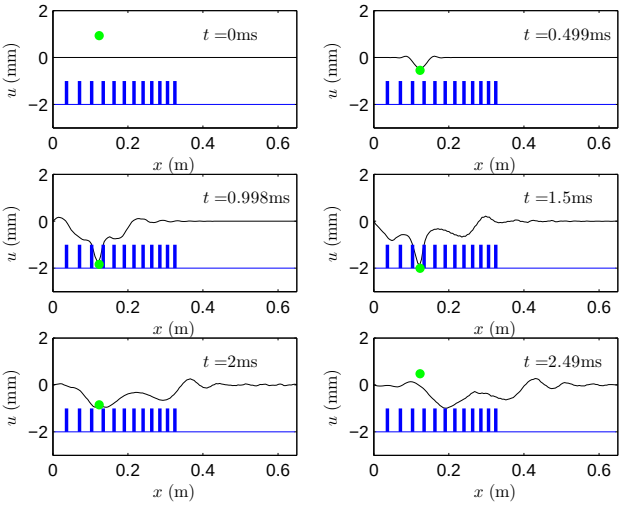

Figure 4: *Collision of an unforced finger (in green), with a string (in black) in contact with a fretboard (in blue). In this case, the string/fretboard parameters are as given in the caption to Figure 2, and the finger is of mass* 5×10^{-3} *kg, and approaches the string with velocity 3 m/s, at a position 0.012 from the end of the string. The finger collision potential parameters are* $K_f = 10^{10}$ *and* $\alpha_f = 2.3$ *and the sample rate is 88.2 kHz.*

particular contact/recontact phenomena visible in the energy of the string/fretboard collision. Energy is conserved to roughly 14 places in this case, as is visible in a plot of the normalized energy variation at right in Figure 5.

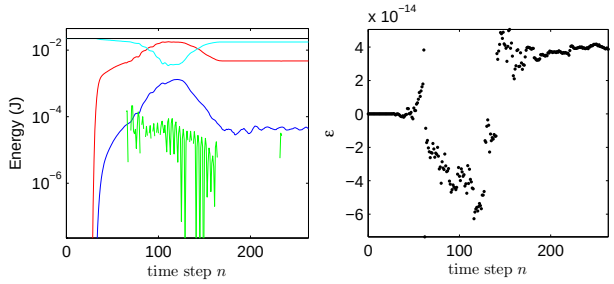

Figure 5: *Left: energy partition for the system of parameters as given in the caption to Figure 4, as a function of time step* n*. Linear string energy* $\mathfrak{h}_L$ *(red), nonlinear string energy* $\mathfrak{h}_K$*, (blue), string/barrier collision energy* $\mathfrak{h}_c$ *(green), finger energy* $\mathfrak{h}_f$ *(cyan) and total energy* $\mathfrak{h}$ *(black). Right: normalized energy variation* $\epsilon = (\mathfrak{h}^{n+1/2} - \mathfrak{h}^{1/2})/\mathfrak{h}^{1/2}$.

4.5. Time-varying Finger Position

As a final example, consider the same system, under the application of a sliding finger stop position—see Figure 6, showing snapshots of the string profile as the finger, under a constant applied force, slides across a single fret, effecting a pitch change. Here, the finger is assumed to act pointwise, at the position as indicated; notice in particular that due to the finite string stiffness, the slope of the string exhibits a strong variation at the fret location, and the minimum may occur at a location slightly shifted from that of the finger.

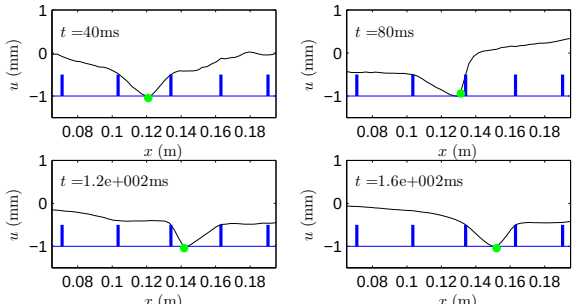

Figure 6: *Time evolution of string profile, for a string/barrier/finger system of parameters as described in the previous sections, where the finger, modelled pointwise, slides over a single fret during a playing gesture.*

5. CONCLUDING REMARKS

This paper is intended as an exploration of various features of string vibration in a more realistic setting, particularly involving the non-trivial contact of various components, including a barrier intended to represent a fretboard. Various features have been neglected here. The most important of these is the modelling of vibration in both polarizations; here, only the polarization transverse to the barrier has been modelled, allowing for an examination in particular of a colliding finger. In the case of excitation in the other polarization, however, a different nonlinear mechanism is required for the finger stopping, which closely resembles that of the bow-string interaction—see [12]. The other important element, not modelled here, is coupling to a body (in the case of, say, an acoustic guitar), and perhaps to the surrounding acoustic space. When such features are included, one is not far from a fully articulated model of a guitar, leaving, then, the enormous problem of gestural control—which is not considered here.

From a numerical point of view, a Hamiltonian potential formulation has been used here in order to arrive at a stable numerical method. As with all such stable methods, this leads to an implicit design in the nonlinear part of the problem (note that the linear part of the scheme, in isolation, remains explicit), and ultimately to a nonlinear vector algebraic equation to be solved at each time step. Though it is possible to show, for very simple systems such as a lumped mass colliding with a rigid barrier [38], and certain extensions to the distributed case [18], that a unique solution exists, in this vector case, a means of showing existence and uniqueness is not immediately forthcoming—meaning that, when an iterative method such as Newton-Raphson is employed it may either (a) not converge, or (b) converge to one solution which may be spurious. Thus an open question, for this and all nontrivial collision problems, is the determination of such uniqueness and existence conditions.

Beyond this basic question, at the level of the iterative solver

employed (in this case, Newton Raphson, but many others are available), there are further issues—one is that, even if existence and uniqueness results are available, convergence of a particular iterative method is not ensured. Another is that, in general, the iterative solver can prove to be something of a bottleneck not merely in terms of the over-all operation count (here, 50 iterations have been employed, for results to machine accuracy, though this can be significantly reduced for audio synthesis), but also in parallel implementations, where reducing the number of iterations (which must be performed serially) is of paramount importance.

6. REFERENCES

[1] J. O. Smith III, *Physical Audio Signal Processing*, Stanford, CA, 2004, Draft version. Available online at `http://ccrma.stanford.edu/~jos/pasp04/`.

[2] V. Välimäki, T. Tolonen, and M. Karjalainen, "Plucked-string synthesis algorithms with tension modulation nonlinearity," in *Proc. IEEE Int. Conf. Acoust., Speech, Sig. Proc.*, Phoenix, Arizona, March 1999, vol. 2, pp. 977–980.

[3] T. Tolonen, V. Välimäki, and M. Karjalainen, "Modeling of tension modulation nonlinearity in plucked strings," *IEEE Transactions on Speech and Audio Processing*, vol. 8, no. 3, pp. 300–310, 2000.

[4] S. Bilbao, "Energy-conserving finite difference schemes for tension-modulated strings," in *Proceedings of the IEEE International Conference on Acoustics, Speech, and Signal Processing*, Montreal, Canada, May 2004, vol. 4, pp. 285–288.

[5] C. Vergez and X. Rodet, "A new algorithm for nonlinear propagation of sound wave: Application to a physical model of a trumpet," *Journal of Signal Processing*, vol. 4, pp. 79–88, 2000.

[6] B. Bank and L. Sujbert, "Generation of longitudinal vibrations in piano strings: From physics to sound synthesis," *J. Acoust. Soc. Am.*, vol. 117, no. 4, pp. 539–557, 2005.

[7] S. Bilbao, "A family of conservative finite difference schemes for the dynamical von Karman plate equations," *Numerical Methods for Partial Differential Equations*, vol. 24, no. 1, pp. 193–216, 2008.

[8] C. Raman, "On some Indian stringed instruments," *Proc. Ind. Assoc. Cult. Sci.*, vol. 7, pp. 29–33, 1922.

[9] J. Kappraff R. Burridge and C. Morshedi, "The sitar string, a vibrating string with a one-sided inelastic constraint," *SIAM J. Appl. Math.*, vol. 42, no. 6, pp. 1231–1251, 1982.

[10] M. Schatzman, "A hyperbolic problem of second order with unilateral constraints: The vibrating string with a concave obstacle," *J. Math. Anal. Appl.*, vol. 73, pp. 138–191, 1980.

[11] A. Krishnaswamy and J. O. Smith III, "Methods for simulating string collisions with rigid spatial obstacles," in *IEEE Workshop on Appl. of Siqnal Processing to Audio and Acoust.*, New Paltz, New York, October 2003, pp. 233–236.

[12] G. Evangelista, "Physical model of the string fret interaction," in *Proc. Int. Conf. Digital Audio Effects*, Paris, France, Sept. 2011, pp. 345–351.

[13] E. Rank and G. Kubin, "A waveguide model for slapbass synthesis," in *Proc. IEEE Int. Conf. Acoust., Speech, Sig. Proc.*, New Paltz, New York, October 1997, pp. 443–446.

[14] S. Siddiq, "A physical model of the nonlinear sitar string," *Arch. Acoust.*, vol. 37, no. 1, pp. 73–79, 2012.

[15] D. Kartofelev, A. Stulov, H.-M. Lehtonen, and V. Välimäki, "Modeling a vibrating string terminated against a bridge with arbitrary geometry," in *Proc. Stockholm Musical Acoust. Conf.*, Stockholm, Sweden, August 2013.

[16] C. Vyasarayani, S. Birkett, and J. McPhee, "Modeling the dynamics of a vibrating string with a finite distributed unilateral constraint: Application to the sitar," *J. Acoust. Soc. Am.*, vol. 125, no. 6, pp. 3673–3682, 2010.

[17] M. Frontini and L. Gotusso, "Numerical study of the motion of a string vibrating against an obstacle by physical discretization," *Appl. Math. Mod.*, vol. 14, pp. 489–494, 1990.

[18] A. Torin S. Bilbao and V. Chatzioannou, "Numerical modelling of collisions in musical instruments," Under review, Acta Acustica united with Acustica. Submitted version available at http://arxiv.org/abs/1405.2589.

[19] G. Evangelista and F. Eckerholm, "Player instrument interaction models for digital waveguide synthesis of guitar: Touch and collisions," *IEEE Transactions on Audio Speech and Language Processing*, vol. 18, no. 4, pp. 822–832, 2010.

[20] G. Cuzzucoli and V. Lombardo, A physical model of the classical guitar, including the player's touch, *Computer Music Journal*, vol. 23, no. 2, pp. 52–69, 1999.

[21] P. Ruiz, "A technique for simulating the vibrations of strings with a digital computer," M.S. thesis, University of Illinois, 1969.

[22] A. Chaigne and A. Askenfelt, "Numerical simulations of struck strings. I. A physical model for a struck string using finite difference methods," *J. Acoust. Soc. Am.*, vol. 95, no. 2, pp. 1112–1118, 1994.

[23] G. Kirchhoff, *Vorlesungen über Mechanik*, Tauber, Leipzig, 1883.

[24] G. F. Carrier, "On the nonlinear vibration problem of the elastic string," *Quarterly of Applied Mathematics*, vol. 3, pp. 157–165, 1945.

[25] T. Hélie and D. Roze, "Sound synthesis of a nonlinear string using Volterra series," *Journal of Sound and Vibration*, vol. 314, no. 1–2, pp. 275–306, 2008.

[26] H. Conklin, "Generation of partials due to nonlinear mixing in a stringed instrument," *J. Acoust. Soc. Am.*, vol. 105, no. 1, pp. 536–545, 1999.

[27] G. Derveaux, A. Chaigne, P. Joly, and E. Bécache, "Time-domain simulation of a guitar: Model and method," *J. Acoust. Soc. Am.*, vol. 114, no. 6, pp. 3368–3383, 2003.

[28] M. Laurson, C. Erkut, V. Välimäki, and M. Kuuskankare, "Methods for modeling realistic playing in acoustic guitar synthesis," *Computer Music Journal*, vol. 25, no. 3, pp. 38–49, 2001.

[29] J. Woodhouse, "On the synthesis of guitar plucks," *Acta Acustica united with Acustica*, vol. 90, pp. 928–944, 2004.

[30] G. Evangelista and J. O. Smith, "Structurally passive scattering element for modeling guitar pluck action," in *Proceedings of the 13th International Digital Audio Effects Conference*, Graz, Austria, September 2010, pp. 10–17.

[31] G. Horvay and A. Veluswami, "Hertzian impact of two elastic spheres in the presence of surface damping," *Acta Mechanica*, vol. 35, pp. 285–290, 1980.

[32] L. Rhaouti, A. Chaigne, and P. Joly, "Time-domain modeling and numerical simulation of a kettledrum," *J. Acoust. Soc. Am.*, vol. 105, no. 6, pp. 3545–3562, 1999.

[33] K. Hunt and F. Crossley, "Coefficient of restitution interpreted as damping in vibroimpact," *ASME J. Appl. Mech.*, pp. 440–5, June 1975.

[34] J. Strikwerda, *Finite Difference Schemes and Partial Differential Equations*, pp. 1–435, SIAM, Philadelphia, 2004.

[35] S. Bilbao, *Numerical Sound Synthesis: Finite Difference Schemes and Simulation in Musical Acoustics*, John Wiley and Sons, Chichester, UK, 2009.

[36] S. Bilbao and J. O. Smith III, "Energy-conserving finite difference schemes for nonlinear strings," *Acta Acustica united with Acustica*, vol. 91, no. 2, pp. 299–311, 2005.

[37] T. Kailath, *Linear Systems*, Prentice Hall, Englewood Cliffs, New Jersey, 1980.

[38] V. Chatziioannou and M. van Walstijn, "An energy conserving finite difference scheme for simulation of collisions.," in *Proc. Stockholm Musical Acoust. Conf.*, Stockholm, Sweden, 2013.